Supporting Information for:

# CYCU-3: An Al(III)-based MOF for $SO_2$ capture and detection

Juan L. Obeso,[a,b,+] Valeria B. López-Cervantes,[a,+] Catalina V. Flores,[a,b,+] Ana Martínez,[c] Yoarhy A. Amador-Sánchez,[b] N.S. Portillo-Velez,[d] Hugo A. Lara-García,[e] Carolina Leyva,[a] Diego Solis-Ibarra[b]* and Ricardo A. Peralta,[d]*

[a]Instituto Politécnico Nacional, CICATA U. Legaria, Laboratorio Nacional de Ciencia, Tecnología y Gestión Integrada del Agua (LNAgua), Legaria 694, Irrigación, 11500, Miguel Hidalgo, CDMX, México

[b]Laboratorio de Fisicoquímica y Reactividad de Superficies (LaFReS), Instituto de Investigaciones en Materiales, Universidad Nacional Autónoma de México, Circuito Exterior s/n, CU, Coyoacán, 04510, Ciudad de México, México.

[c]Departamento de Materiales de baja Dimensionalidad. Instituto de Investigaciones en Materiales, Universidad Nacional Autónoma de México. Circuito Interior SN, Ciudad Universitaria, CP 04510, Coyoacán, CDMX, México.

[d]Instituto de Física, Universidad Nacional Autónoma de México, Apartado Postal 20-364, Mexico City 0100, Mexico.

[e]Departamento de Química, División de Ciencias Básicas e Ingeniería. Universidad Autónoma Metropolitana (UAM-I), 09340, México.

[+]These authors contributed equally to this work.

**Table of contents**

## S1. Experimental details

### Analytical instruments

### Powder X-Ray Diffraction Patterns (PXRD)

Using a nickel filter, PXRD was recorded on a D-5000 Diffractometer, Ultima IV, with Cu-Kα1 radiation (λ = 1.5406 Å). The patterns were recorded in the 2θ range 2–50° with a step scan of 0.02° and a scan rate of 0.05° $min^{-1}$.

### Fourier-transform infrared spectroscopy (FT-IR)

FT-IR spectra were obtained in the 4000-500 $cm^{-1}$ range on a Shimadzu IRTracer-100 spectrometer with a Golden Gate Single Reflection diamond ATR cell.

### Thermal gravimetric analysis (TGA)

TGA was performed using a TA Instruments Q500HR analyzer under an $N_2$ atmosphere using the high-resolution mode (dynamic rate TGA) at a scan rate of 5 °C $min^{-1}$, from room temperature to 800 °C.

### Solid-State Ultraviolet-visible spectroscopy (UV-Vis)

Absorption measurements were performed from 200-800 nm using a Shimadzu spectrophotometer UV-2600 equipped with an ISR-2600Plus integrating sphere and a $BaSO_4$ blank.

### Fluorescence spectroscopy

Emission spectra were taken in an Edinburgh Instrument FS5 fluorimeter using a continuous wave 150 W ozone-free xenon arc lamp at room temperature. For the emission experiments, the solid samples were slightly ground in an agate mortar to homogenize the microcrystals. They were later packed into the quartz sample holders and positioned in the instrument. Measurements were carried out using an excitation wavelength of 343 nm, with an additional 345 nm high pass on the detector side to remove any remnant light from the excitation source. The measurements were collected with a step size of 0.3 nm, a dwell time of 0.50 s, and two runs for every scan. The excitation bandwidth was set at 0.10 nm, and the emission bandwidth for the detector at 3.00 nm.

## S2. Results and Discussion

### Synthesis of CYCU-3

### PXRD

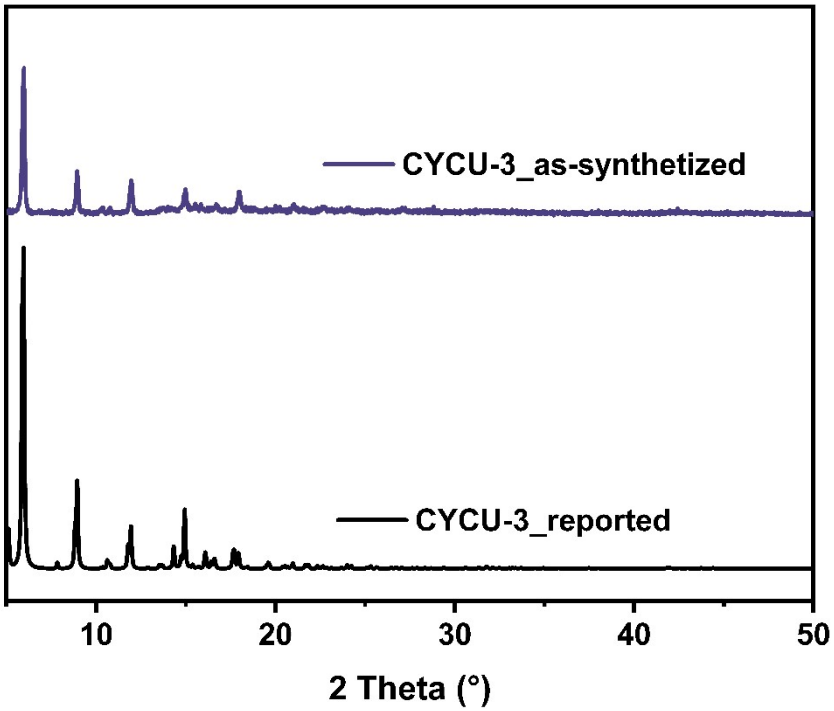


**Figure S1.** PXRD patterns of CYCU-3 reported, and CYCU-3 as-synthetized.

**FT-IR**

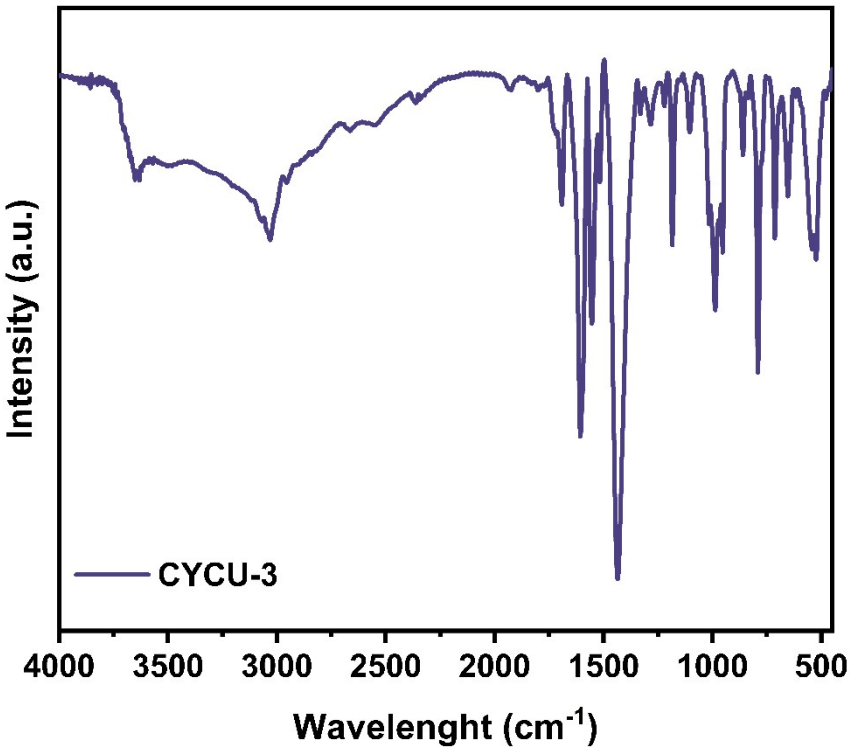


**Figure S2.** FTIR spectra of CYCU-3 as-synthetized.

**TGA**

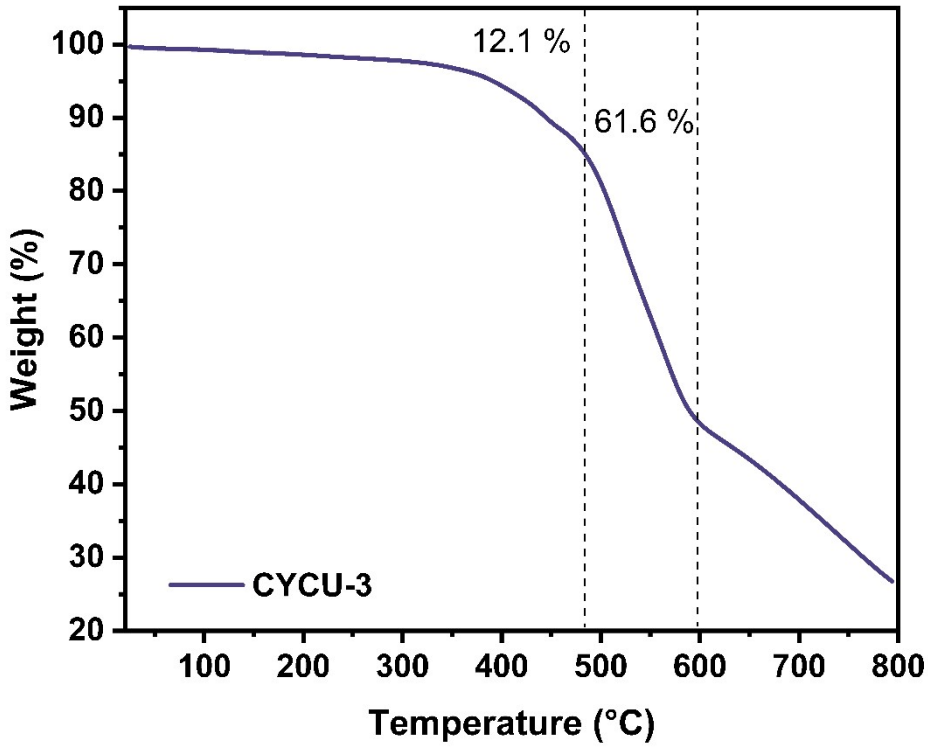


**Figure S3.** TGA analysis profile of CYCU-3 as-synthetized.

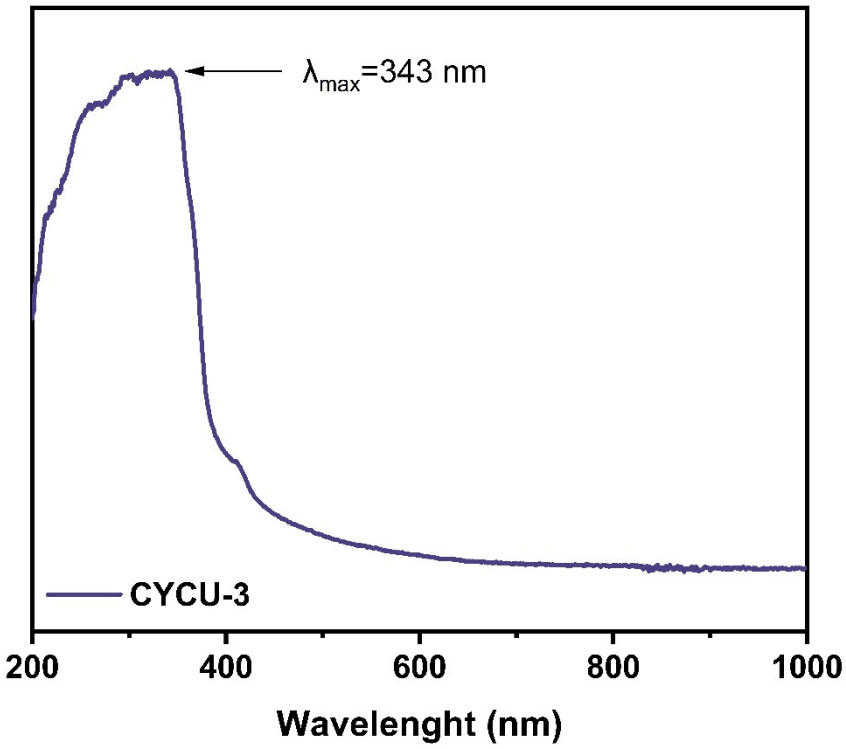


**Figure S4**. Solid-state UV-Vis spectra of CYCU-3 as-synthetized.

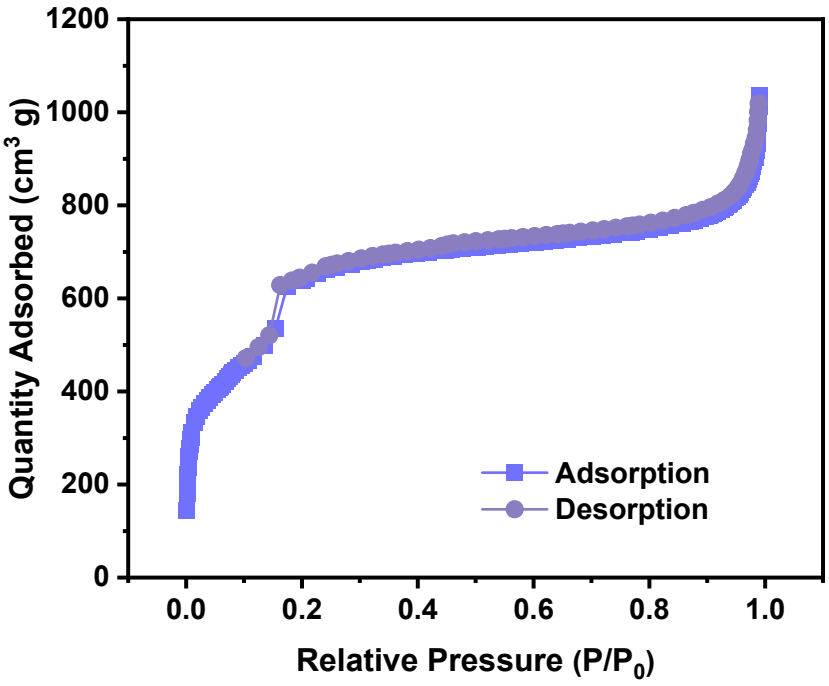


**Figure S5**. Nitrogen isotherm at 77 K of CYCU-3 as-synthetized.

**Gases Adsorption experiments**

| **Table S1.** Comparison of $SO_2$ uptake at 1 bar for different Al(III)-based MOFs. | | | | | |
|---|---|---|---|---|---|
| MOFs | Vp ($cm^3g^{-1}$) | BET ($m^2 g^{-1}$) | $SO_2$ uptake (mmol $g^{-1}$) | Temperature (K) | Ref. |
| CYCU-3 | 1.36 | 2711 | 11.03 | 298 | This work |
| MOF-303 | 0.58 | 1211.78 | 7.86 | 298 | [1] |
| MIL-53(Al)-TDC | 0.45 | 1260 | 8.9 | 298 | [2] |
| MIL-53(Al)-BDC | 0.51 | 1210 | 10.8 | 298 | |
| MIL-100(Al) | 0.824 | 1890 | 16.3 | 293 | [3] |
| MIL-96 | 0.24 | 530 | 6.5 | 293 | |
| DUT-4 | 0.71 | 1348 | 13.6 | 298 | [4] |
| MIL-160 | 0.46 | 1170 | 7.2 | 293 | [5] |
| CAU-23 | 0.51 | 1176 | 8.4 | 293 | [6] |
| CAU-10 | 0.25 | 630 | 4.47 | 298 | [7] |

## CYCU-3 after $SO_2$ adsorption experiments

### PXRD patterns after dry $SO_2$ adsorption and after wet $SO_2$ exposure

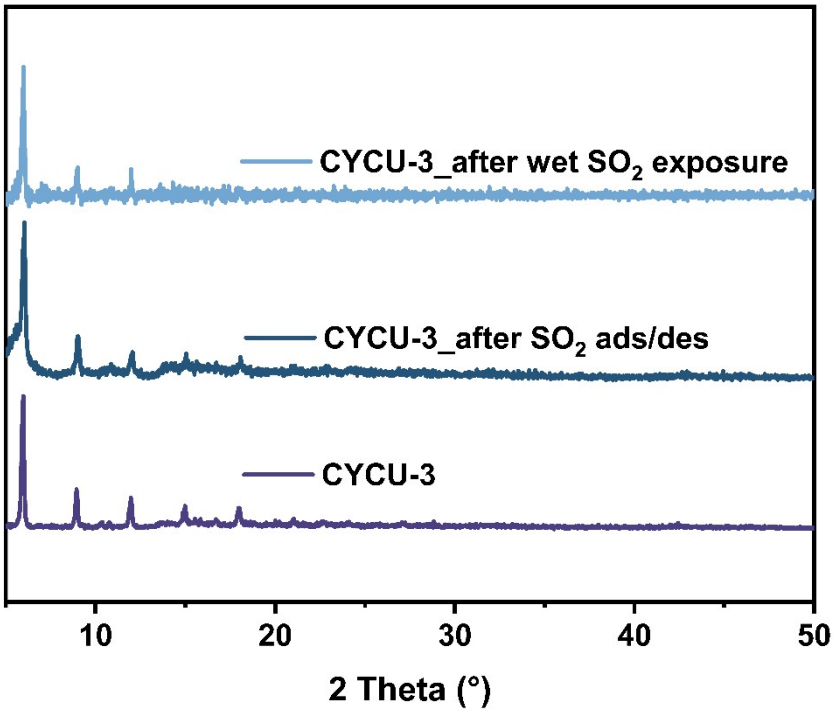


**Figure S6.** PXRD patterns of CYCU-3: as-synthetized, after dry $SO_2$ adsorption and wet $SO_2$ exposure.

**Nitrogen isotherm after $SO_2$ experiments**

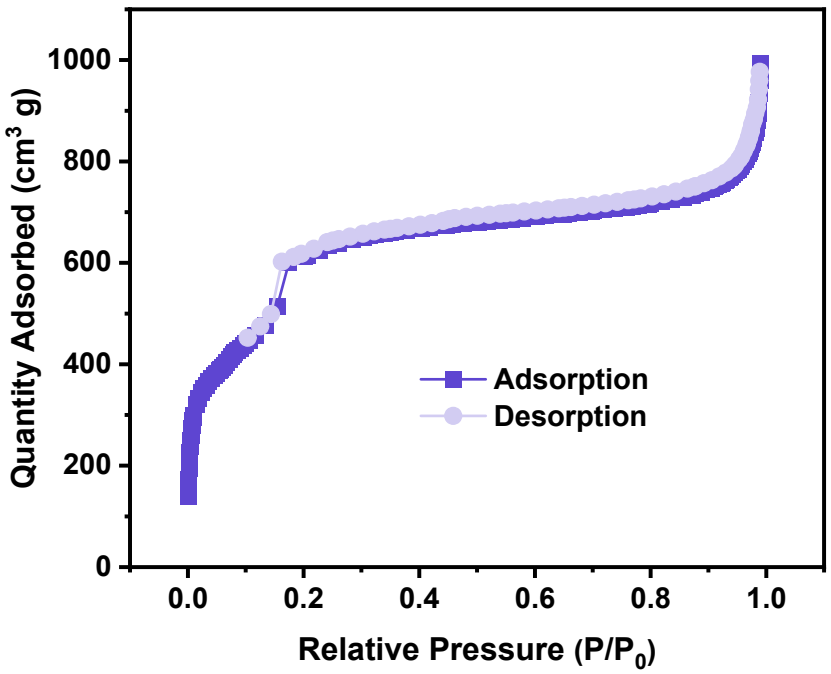


**Figure S7**. Nitrogen isotherm at 77 K of CYCU-3 after $SO_2$ experiments

**Isosteric heat of $SO_2$ adsorption experiments**

The heat of adsorption of CYCU-3 was calculated accordingly to the reported literature,[8] using a virial-type equation (Eq. S1) to fit the low coverage region of two adsorption isotherms at 298 and 303 K (Figure S8).

$$\text{Ln}\,(n/p) = A_0 + A_1\eta + A_2\eta^2 + \cdots \qquad \text{Eq. S1}$$

Where p is the pressure in kPa, n is the amount adsorbed and $A_0$, $A_1$, … are the virial coefficients. The plot *Ln (P) vs. n* can fit both isotherms simultaneously (Figure S9). From the linear fittings, the virial coefficients are used to estimate the enthalpy of adsorption.

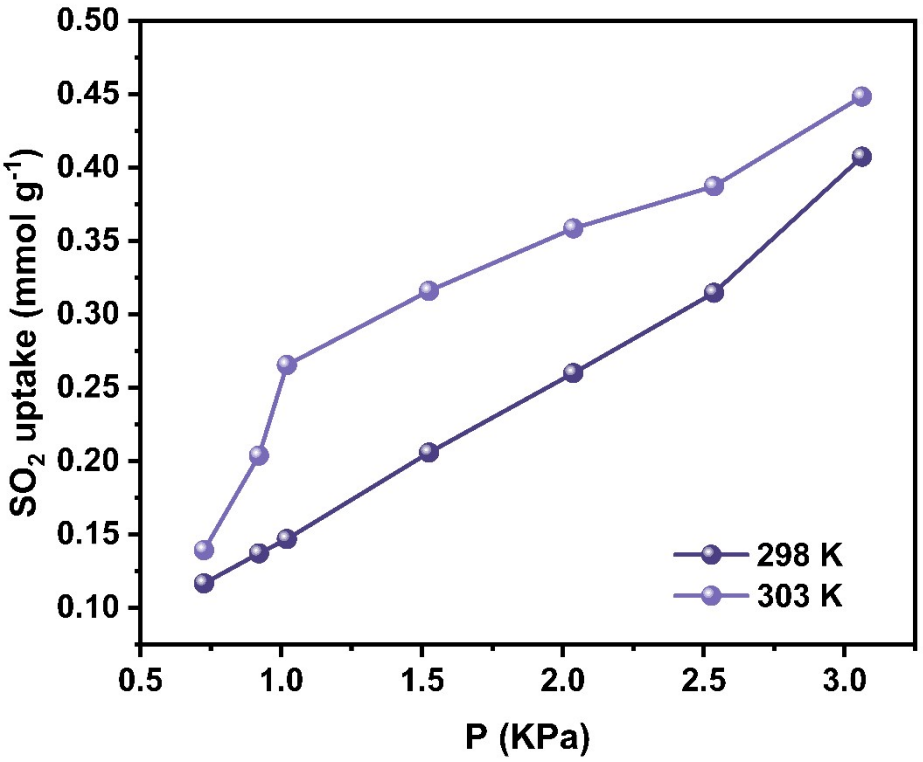


**Figure S8.** $SO_2$ adsorption isotherms of CYCU-3 at 298 and 303 K.

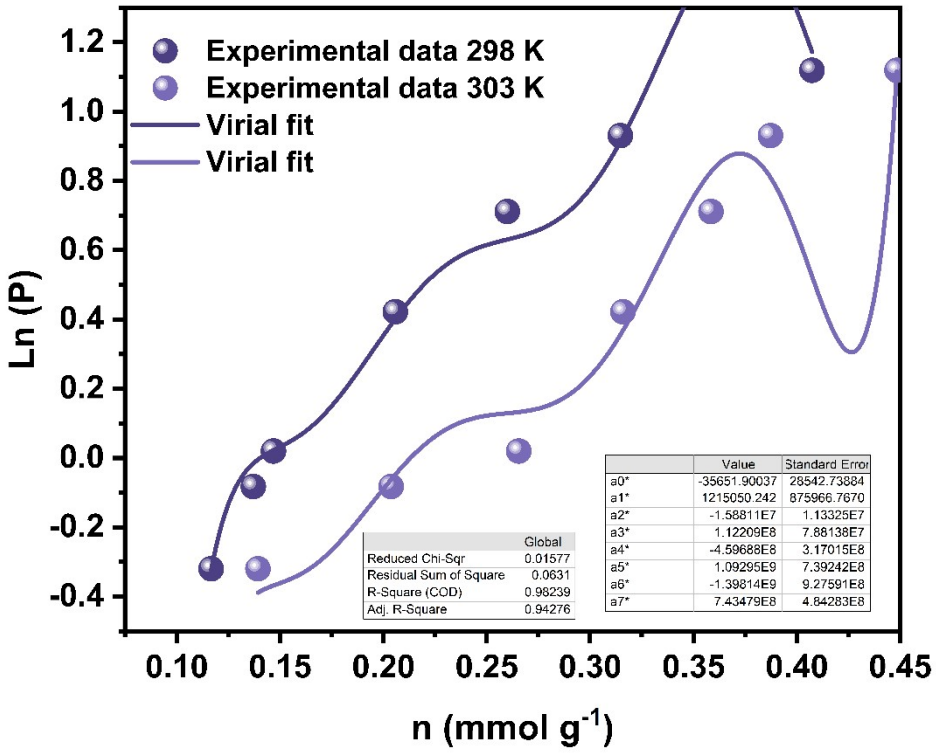


**Figure S9**. Virial fitting plots for the adsorption isotherms of $SO_2$ for CYCU-3.

**System for ex situ wet $SO_2$ exposure experiments**

The system (Figure S10) contains two principal parts:

A. The gas generator, in which $Na_2SO_3$ is added to a two-neck ball flask [1], of which is capped with a rubber stopper through which $Na_2SO_3$ is injected with a syringe [2]. One of which is covered with a rubber stopper through which concentrated $H_2SO_4$ is injected with a glass syringe [2], while the other is covered with a rubber stopper [3]. Concentrated $H_2SO_4$ [2] is injected through a glass syringe while the other port is connected to the saturation chamber. saturation chamber.

B. The saturation chamber, made of a round flask [3], is connected to a vacuum line [4] and a vacuum line [4]. vacuum line [4] and a pressure gauge [5].

To start the process, a sample of about 20 mg in a 1.5 mL glass vial was activated in a sand bath at 423 K under vacuum for 24 h. The sample was then placed in the saturation chamber, and the system was evacuated with a vacuum line. The vial was then placed in the saturation chamber, and the system was evacuated with a vacuum line. Next, 1 bar of $SO_2$ gas was generated by dripping 1.2 mL of concentrated $H_2SO_4$ over 2 g of $Na_2SO_3$, the sample was left continuously exposed to the gas for 3 hours. For the sample exposed to 0.1 bar $SO_2$, the sample was activated in the same way, and 0.12 mL of concentrated $H_2SO_4$ was dripped onto 0.2 g of $Na_2SO_3$. The sample was left continuously exposed to the gas for 3 hours.

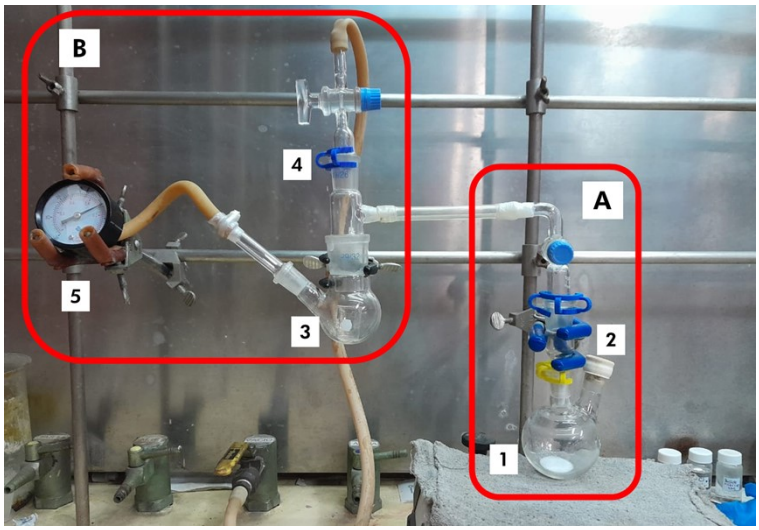


**Figure S10.** Homemade system for wet $SO_2$ adsorption experiments.

## $SO_2$ computational chemistry

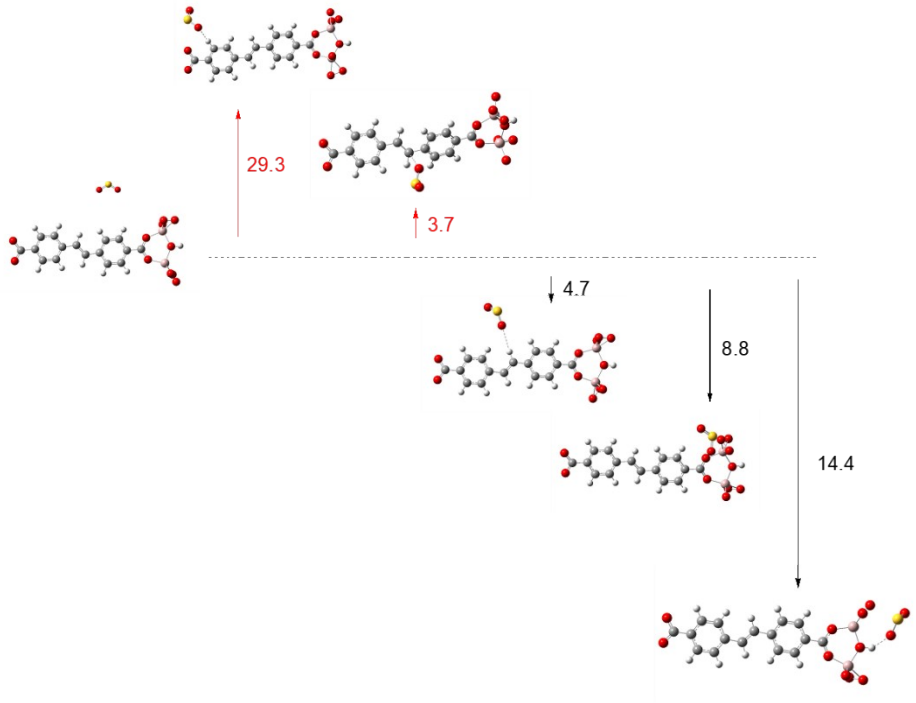


**Figure S11.** Partial optimization of $SO_2$ molecule interaction with five different positions in CYCU-3.

**Fluorescence experiments**

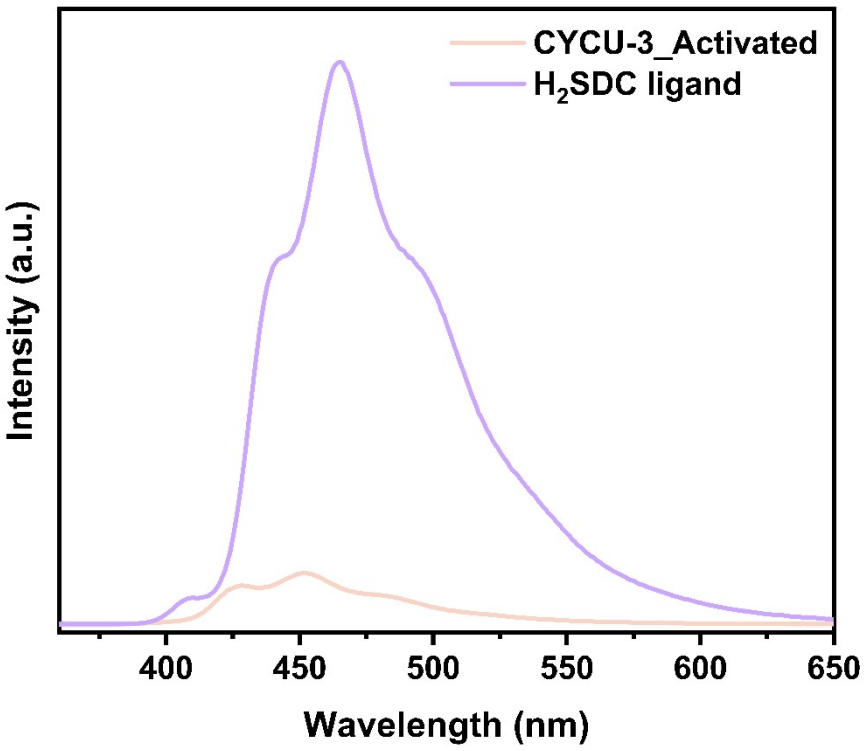


**Figure S12.** Solid-State emission spectra of $H_2$SDC linker and CYCU-3 activated.

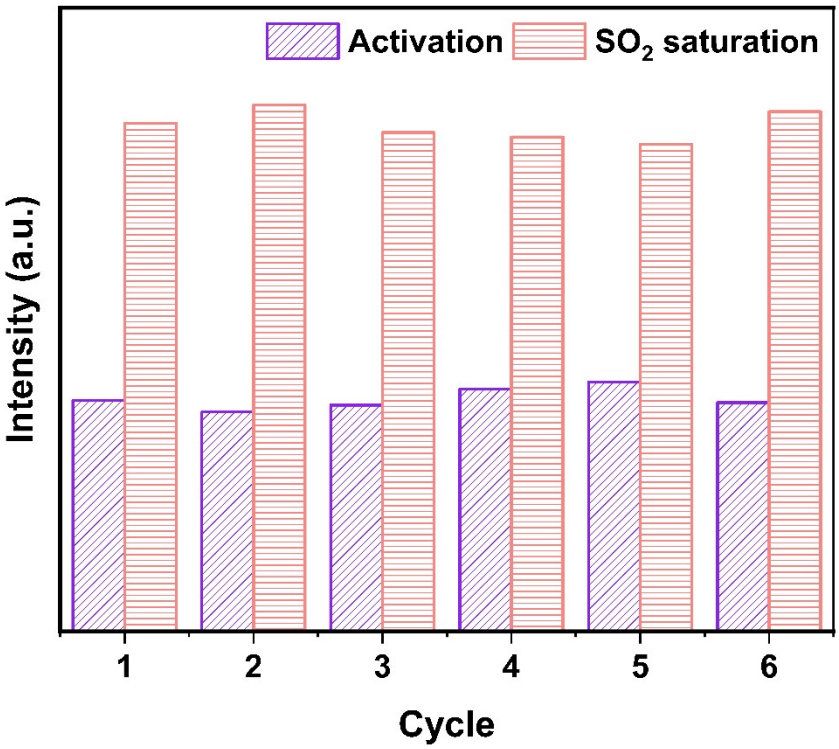


**Figure S13.** Photoluminescence intensity of activated and $SO_2$-saturated cycles of a CYCU-3 sample.

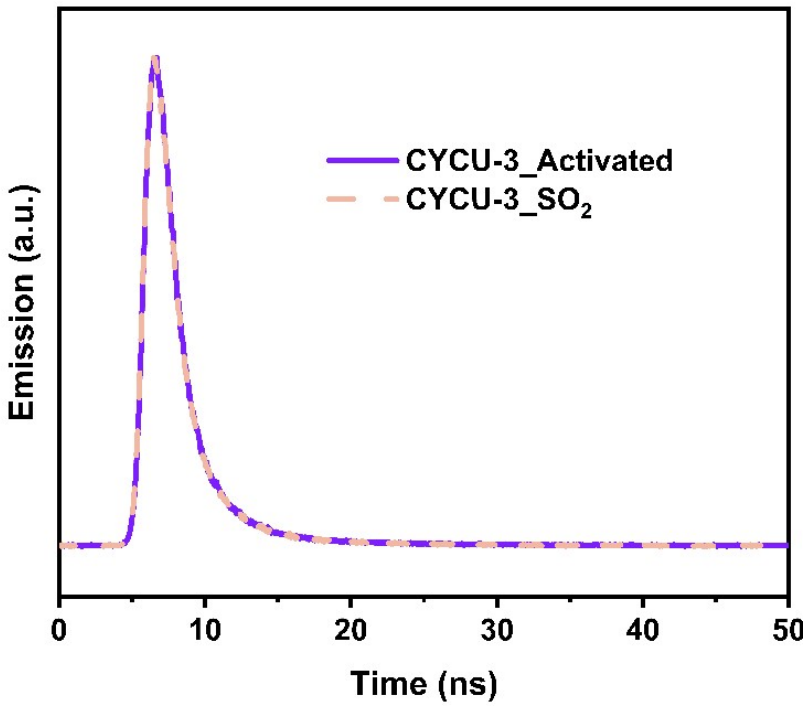

**Figure S14.** Time-resolved photoluminescence decay spectra of activated CYCU-3 and $SO_2$-saturated CYCU-3 measured at 450 nm emission.

| **Table S2.** Average decay lifetime for CYCU-3. | | | | |
|---|---|---|---|---|
| **Sample** | **$\tau_1$ (ns)** | **$\tau_2$ (ns)** | **$\tau_3$ (ns)** | **Fluorescence lifetime (ns)** |
| **Activated** | 0.8508 | 1.1969 | 8.4462 | **2.20766** |
| **$SO_2$ saturated** | 0.6226 | 1.6658 | 6.9300 | **2.08989** |

## S4. References


(1) Obeso, J. L.; Martínez-Ahumada, E.; López-Olvera, A.; Ortiz-Landeros, J.; Lara-García, H. A.; Balmaseda, J.; López-Morales, S.; Sánchez-González, E.; Solis-Ibarra, D.; Leyva, C.; Ibarra, I. A. MOF-303 as an Effective Adsorbent to Clean $CH_4$: $SO_2$ Capture and Detection. *ACS Appl. Energy Mater.* **2022**. https://doi.org/10.1021/acsaem.2c02983.

(2) López-Olvera, A.; Zárate, J. A.; Martínez-Ahumada, E.; Fan, D.; Díaz-Ramírez, M. L.; Sáenz-Cavazos, P. A.; Martis, V.; Williams, D. R.; Sánchez-González, E.; Maurin, G.; Ibarra, I. A. $SO_2$ Capture by Two Aluminum-Based MOFs: Rigid-like MIL-53(Al)-TDC versus Breathing MIL-53(Al)-BDC. *ACS Appl. Mater. Interfaces* **2021**, *13* (33), 39363–39370. https://doi.org/10.1021/acsami.1c09944.

(3) Brandt, P.; Xing, S.-H.; Liang, J.; Kurt, G.; Nuhnen, A.; Weingart, O.; Janiak, C. Zirconium and Aluminum MOFs for Low-Pressure $SO_2$ Adsorption and Potential Separation: Elucidating the Effect of Small Pores and $NH_2$ Groups. *ACS Appl. Mater. Interfaces* **2021**, *13* (24), 29137–29149. https://doi.org/10.1021/acsami.1c06003.

(4) López-Olvera, A.; Pioquinto-García, S.; Antonio Zárate, J.; Diaz, G.; Martínez-Ahumada, E.; Obeso, J. L.; Martis, V.; Williams, D. R.; Lara-García, H. A.; Leyva, C.; Soares, C. V.; Maurin, G.; Ibarra, I. A.; Dávila-Guzmán, N. E. $SO_2$ Capture in a Chemical Stable Al(III) MOF: DUT-4 as an Effective Adsorbent to Clean $CH_4$. *Fuel* **2022**, *322*, 124213. https://doi.org/10.1016/j.fuel.2022.124213.

(5) Brandt, P.; Nuhnen, A.; Lange, M.; Möllmer, J.; Weingart, O.; Janiak, C. Metal–Organic Frameworks with Potential Application for $SO_2$ Separation and Flue Gas Desulfurization. *ACS Appl. Mater. Interfaces* **2019**, *11* (19), 17350–17358. https://doi.org/10.1021/acsami.9b00029.

(6) Jansen, C.; Tannert, N.; Lenzen, D.; Bengsch, M.; Millan, S.; Goldman, A.; Jordan, D. N.; Sondermann, L.; Stock, N.; Janiak, C. Unravelling Gas Sorption in the Aluminum Metal-organic Framework CAU-23: $CO_2$, $H_2$, $CH_4$, $SO_2$ Sorption Isotherms, Enthalpy of Adsorption and Mixed-adsorptive Calculations. *Zeitschrift für Anorg. und Allg. Chemie* **2022**, *648* (17). https://doi.org/10.1002/zaac.202200170.

(7) Zárate, J. A.; Domínguez-Ojeda, E.; Sánchez-González, E.; Martínez-Ahumada, E.; López-Cervantes, V. B.; Williams, D. R.; Martis, V.; Ibarra, I. A.; Alejandre, J. Reversible and Efficient $SO_2$ Capture by a Chemically Stable MOF CAU-10: Experiments and Simulations. *Dalt. Trans.* **2020**, *49* (27), 9203–9207. https://doi.org/10.1039/D0DT01595D.

(8) Nuhnen, A.; Janiak, C. A Practical Guide to Calculate the Isosteric Heat/Enthalpy of Adsorption via Adsorption Isotherms in Metal–Organic Frameworks, MOFs. *Dalt. Trans.* **2020**, *49* (30), 10295–10307. https://doi.org/10.1039/D0DT01784A.